

## **Pegmatite-wallrock interaction: Holmquistite-bearing amphibolite, Edison pegmatite, Black Hills, South Dakota**

**C. K. SHEARER, J. J. PAPIKE**

Institute for the Study of Mineral Deposits, South Dakota School of Mines and Technology,  
Rapid City, South Dakota 57701, U.S.A.

### **ABSTRACT**

The fluid transport of relatively incompatible elements (Li, Rb, Cs) out of the rare-element pegmatite system and the subsequent interaction between that fluid and amphibolite result in the stabilization of holmquistite-bearing assemblages. In the amphibolite adjacent to the Edison pegmatite, Black Hills, South Dakota, three amphibolite assemblages resulting from fluid–country rock interaction can be distinguished: (1) biotite alteration assemblage, (2) hornblende-holmquistite alteration assemblage, and (3) hornblende-plagioclase assemblage.

Holmquistite occurs only in assemblages 1 and 2 in which it coexists with and partially replaces hornblende. In coexisting holmquistite-hornblende pairs, the  $(Al + Fe^{3+} + 2Ti^{4+})$  value is greater, and the  $(Fe^{2+} + Mn)/(Fe^{2+} + Mn + Mg)$  ratio is less in holmquistite than in coexisting hornblende. By analogy to calcic and Fe-Mg amphiboles, a wide compositional gap exists between calcic and Li-rich amphiboles at temperatures of alteration-zone formation.

The alteration of the amphibolite appears to be the result of (1) Li and K metasomatic alteration by alkali-rich, pegmatite-derived aqueous fluids and (2) retrograde metamorphism by the aqueous fluids resulting in the instability of plagioclase and ilmenite and the formation of epidote and sphene. The fluid has low B and F concentrations relative to fluids derived from lepidolite-bearing pegmatites in the same region. The conditions at which the alteration occurred were between 510 and 350 °C at 3–4 kbar. Field and textural evidence cannot discriminate between a single fluid–amphibolite interaction model and a multiple fluid–amphibolite interaction model.

### **INTRODUCTION**

Because of the enrichment of pegmatitic magma and coexisting aqueous fluid in relatively incompatible elements such as Li, Rb, Cs, B, Ta, and Nb, fluid transport of these constituents out of the rare-element pegmatite system and subsequent interaction between that fluid and country rock result in the modification of the composition of the primary minerals or stabilization of exotic mineral assemblages. The composition of the fluid phase is a function of magma composition, and therefore the diagnostic elements of the alteration aureoles are related to pegmatite type (Beus, 1960) and provide a valuable exploration tool (Beus, 1960; Truman and Černý, 1982; Norton, 1984; London, 1986). In addition to utilization for pegmatite exploration, the chemical and mineralogical characteristics of exomorphic aureoles surrounding rare-element pegmatites also provide (1) valuable information concerning pegmatite fluid composition (Shearer et al., 1985, 1986; Walker, 1984), (2) a natural analogue for the processes of elemental migration over geologic time scales and in natural geologic environments, and (3) a natural laboratory for the study of crystal-chemical behavior and phase equilibria through the natural addition of high concentrations of incompatible elements (Li, Rb,

Cs, B, F) to primary metamorphic assemblages (Shearer et al., 1986).

Mineral assemblages and element partitioning between coexisting minerals in altered micaeous schist surrounding rare-element pegmatites have been studied in a number of pegmatite fields. The alteration assemblages are most commonly a series of tourmaline-rich assemblages resulting from the transport of B into the schist country rock (Page et al., 1953; Shearer et al., 1984, 1986) and/or a series of retrograde metamorphic assemblages resulting from low-temperature re-equilibration of primary metamorphic assemblages with pegmatite-derived aqueous solutions (Shearer et al., 1986). Sheet silicates in these alteration assemblages are commonly enriched in alkali elements. The partitioning of alkali elements between coexisting sheet silicates in these alteration zones appears to be well defined and can be rationalized in terms of crystal-chemical behavior (Papike et al., 1984; Shearer et al., 1986).

Although less common, holmquistite-bearing assemblages resulting from the interaction of pegmatite-derived fluids and amphibolite have been described by several researchers and summarized by Heinrich (1965) and London (1986). These summary papers (Heinrich, 1965; London, 1986) cited the following characteristics of

holmquistite-bearing assemblages: (1) holmquistite assemblages reflect greenschist facies metamorphic conditions; (2) holmquistite is found only in amphibolite wall-rock usually replacing hornblende, pyroxene, or biotite, and its formation is a function of the activity of Li species introduced into the amphibole wall zone; (3) holmquistite is formed around Li rich pegmatites in which spodumene, lepidolite–lithian muscovite, or petalite are stable lithium aluminosilicates; and (4) the formation of holmquistite assemblages in the amphibolite country rock is not restricted to early episodes of pegmatite fluid–amphibolite interaction but may form at any time from pegmatite injection to final consolidation.

Mineral assemblages in these amphibolite alteration zones have been described (London, 1986; Nickel et al., 1960; Wright, 1963; Karpoff, 1960; Heinrich, 1965; Osann, 1913; Sundius, 1947); however, with the exception of studies by von Knorring and Hornung (1961) and Wilkins et al. (1970), the variation in mineral chemistries, mineral assemblages, and chemographic relations has not been documented. In addition, the fluid–amphibolite interactions have not been considered in previous studies. This study emphasizes the use of the amphibolite alteration zone adjacent to the Edison pegmatite, Black Hills, South Dakota, to assess the effect of pegmatite fluid–amphibolite interaction on mineral assemblage, mineral chemistry, and phase relations.

#### GEOLOGY OF THE EDISON PEGMATITE AND ADJACENT COUNTRY ROCK

The Edison pegmatite is located approximately 1.2 km southeast of Keystone, South Dakota (Fig. 1A). The pegmatite is spatially and presumably genetically related to the surrounding Harney Peak Granite [approximately 1.7 Ga (Riley, 1970; Z. Peterman, pers. comm., 1986)]. The pegmatite field has been classified as a rare-element type with mineralogical characteristics ranging from barren to Li-, Rb-, Cs-, Be-, Ta-, and Nb-enriched types (Černý, 1982). The Edison pegmatite is a complex, irregular-shaped body consisting of two mineralogically and texturally distinct zones. The wall zone of the pegmatite consists of albite-quartz assemblages with variable amounts of muscovite, beryl, microcline, lithiophilite-triophyllite, columbite-tantalite, apatite, and tourmaline. Quartz-spodumene-albite mineral assemblages, which occur as four separate bodies within the pegmatite, represent the second zone. The spodumene-bearing bodies are separated by the wall-zone assemblage. The quartz-spodumene-albite assemblage grades inward to a quartz-spodumene assemblage (Page et al., 1953).

The Edison pegmatite intrudes amphibolite, iron formation (grunerite schist and quartzite) and mica-garnet schist country rock (Fig. 1B). Foliation is poorly developed in the amphibolite, and the pegmatite follows fractures across the amphibolite. However, in other lithologies, the pegmatite follows bedding or foliation planes within the schist or the contacts between lithologic units.

TABLE 1. Typical mode (in wt%) of mineral assemblages

|              | ED1   | ED3   | ED5   |
|--------------|-------|-------|-------|
| Quartz       | 20.0  | 16.9  | 7.0   |
| Plagioclase  | 0.0   | 4.2   | 23.2  |
| Hornblende   | 6.0   | 47.3  | 67.3  |
| Biotite      | 20.0  | 0.4   | 0.1   |
| Holmquistite | 35.8  | 18.6  | 0.0   |
| Epidote      | 9.1   | 6.5   | 0.0   |
| Chlorite     | 4.4   | 4.4   | 0.0   |
| Ilmenite     | 0.0   | 0.5   | 2.4   |
| Pyrite       | 1.5   | 1.1   | 0.0   |
| Sphene       | 3.2   | 0.0   | 0.0   |
| Total        | 100.0 | 100.0 | 100.0 |

Diamond-drill data has been interpreted to indicate that the pegmatite is located on the limb of a large isoclinal fold. Minor folds control the shape of the eastern pegmatite contact (Page et al., 1953). The geology of the Edison pegmatite has been discussed in detail by Page et al. (1953).

#### ANALYTICAL TECHNIQUES

Thin sections of the amphibolite were studied with a Zeiss photomicroscope equipped with both transmitted- and reflected-light optics. Modal data were collected with a Swift automated point counter set for a grid spacing of 150  $\mu\text{m}$ . Minerals in the amphibolite were analyzed for nine major and minor elements by microprobe techniques using the fully automated Materials Analysis Company electron microprobe at the South Dakota School of Mines and Technology. A wavelength-dispersive system with TAP, PET, and LIF crystals was utilized for quantitative determination of Si, Ti, Al, Fe, Mg, Mn, Ca, Na, and K. All analyses were conducted at an accelerating voltage of 15 kV, a beam current of approximately 0.0150 A, and a counting time of 20000 counts or 20 s. Corrections were made with the Bence-Albee empirical correction technique (Bence and Albee, 1968).

Clean mineral separates (hornblende, holmquistite, biotite) were prepared using a combination of hand-picking, magnetic separation, and heavy-liquid separation techniques.  $\text{Fe}^{2+}$  determinations were conducted using a potassium permanganate titration technique (Goldich, 1984).  $\text{Fe}^{3+}$  was calculated as the difference between microprobe (total Fe) and wet-chemical ( $\text{Fe}^{2+}$ ) results. Li was determined by atomic absorption spectrometry using a Perkin-Elmer 5500 AA-ICP. F was determined by standard electrode technique, and  $\text{H}_2\text{O}$  was calculated by subtracting F from total loss on ignition. In addition to optical identification, holmquistite was also identified using powder X-ray diffraction techniques. Cell refinement of the holmquistite (sample ED1A) was determined using the OCELRF program written by C. T. Prewitt. Fifteen diffraction peaks from an indexed powder pattern were used in calculating cell parameters.

Amphibole structural formulae were calculated from combined microprobe and wet-chemical analyses using cation-site assignment criteria suggested by Robinson et al. (1982). Amphibole structural formulae were calculated on the basis of 46 negative charges. Biotite structural formulae were calculated on the basis of 44 negative charges.

Major and trace elements in the amphibolite were analyzed by energy-dispersive XRF (Battelle) and ICP and AA (South Dakota School of Mines and Technology).  $\text{SiO}_2$ ,  $\text{TiO}_2$ ,  $\text{Al}_2\text{O}_3$ ,  $\text{FeO}$ ,  $\text{MnO}$ ,  $\text{CaO}$ ,  $\text{K}_2\text{O}$ , Ga, Cu, Nb, U, and Y were analyzed by XRF. Remaining elements in Table 2 were analyzed by ICP and AA. Rock powders used in the major- and trace-element analyses

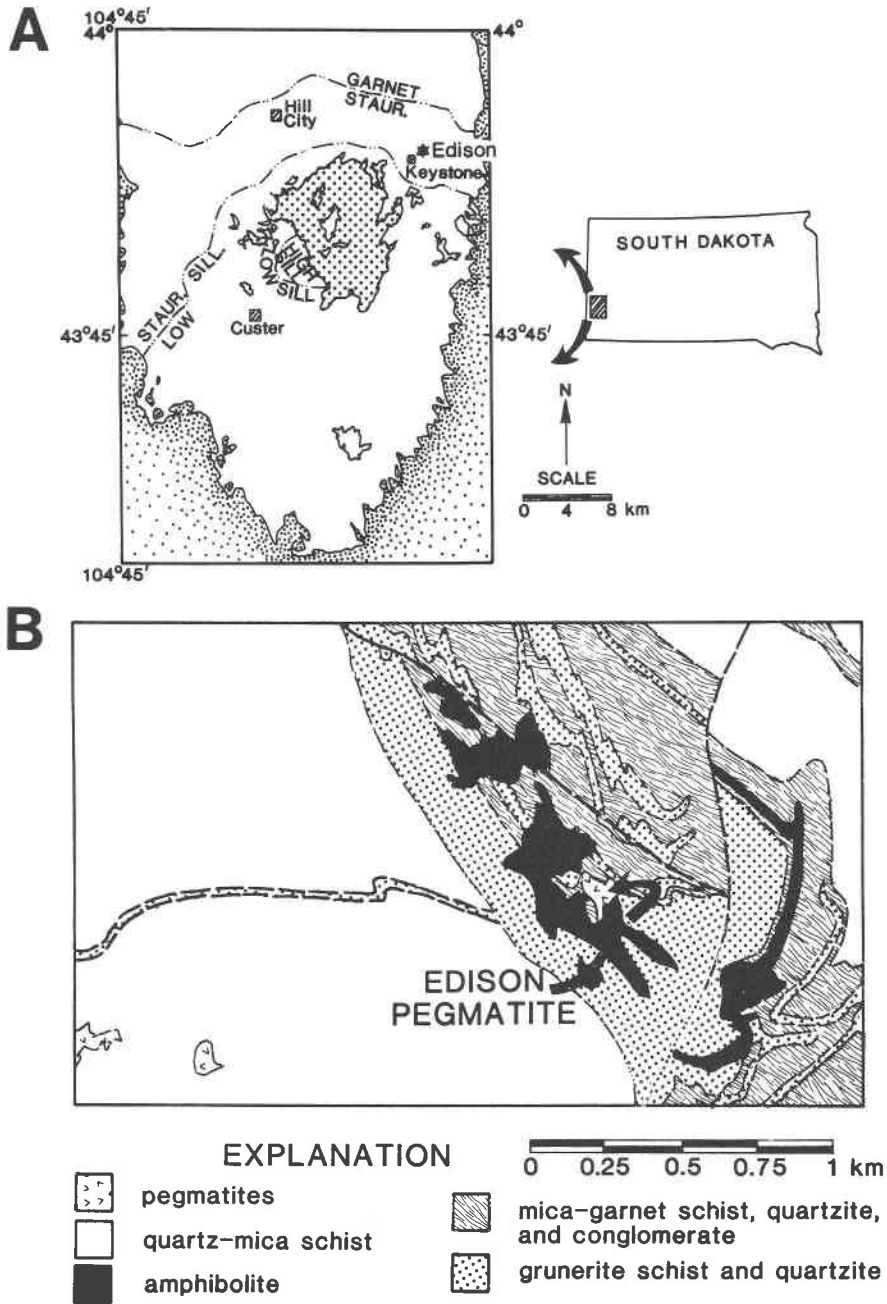


Fig. 1. (A) Location of the Edison pegmatite within the southern portion of the Precambrian core of the Black Hills uplift, to the northeast of the Harney Peak Granite. (B) Bedrock geologic map of the area surrounding the Edison pegmatite (modified from Norton, 1976).

were also used to determine quantitative modes by the reference intensity method (RIM). This multicomponent X-ray diffraction analysis can be performed with acceptable accuracy, providing that preferred orientation and absorption errors can be minimized. This is accomplished in the RIM procedure by reducing the particle size of the sample material to values in the 5- to 15- $\mu$ m-diameter range and by suspending the sample as an aerosol in an aspirator jar and collecting the aerosol particles on an amorphous fiber filter substrate. Summary of the RIM procedure

is given by Davis (1978, 1980). RIM-XRD modes for samples ED1, ED3, and ED5 are given in Table 1.

**AMPHIBOLITE ALTERATION MINERAL ASSEMBLAGES**

The metasomatic alteration zone in the amphibolite adjacent to the Edison pegmatite can be divided into three mineral assemblages: (1) biotite alteration assemblage; (2) hornblende-holmquistite alteration assemblage; and (3)

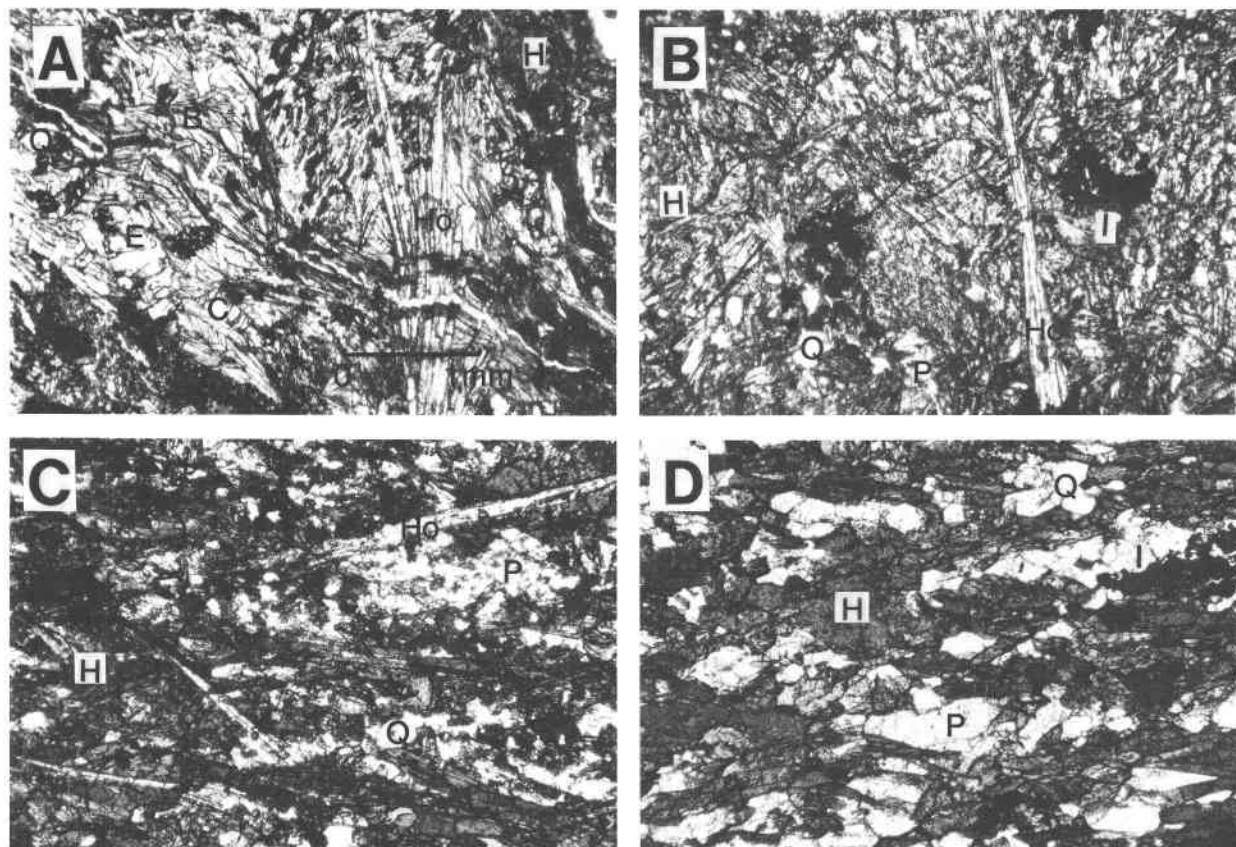


Fig. 2. Photomicrographs of amphibolite within the alteration zone adjacent to the Edison pegmatite. (A) Biotite alteration zone. (B) Hornblende-holmquistite alteration zone. Illustrates holmquistite cutting across hornblende. (C) hornblende-holmquistite alteration zone. Illustrates holmquistite parallel to hornblende elongation. (D) Hornblende-plagioclase assemblage. Ho = holmquistite, H = hornblende, P = plagioclase, I = ilmenite, Q = quartz, B = biotite, E = epidote, and C = calcite. Scale on 2A.

hornblende-plagioclase assemblage. The typical modal mineralogy of each assemblage is presented in Table 1. The amphibolite, which is primarily exposed along the footwall of the pegmatite, shows varying degrees of alteration. The biotite alteration assemblage is always spatially situated between the wall zone of the pegmatite and the hornblende-holmquistite alteration zone.

The biotite alteration assemblage consists of biotite + holmquistite + quartz + hornblende (<3%) + epidote + sphene (<1%), + pyrite (<1%) + calcite (<1%). The rocks of this assemblage are fine grained (average 100  $\mu\text{m}$ ) and consist of minor amounts of medium-grained, partially replaced hornblende (485  $\mu\text{m}$ ) interspersed in a fine-grained matrix consisting predominantly of biotite, epidote, quartz, and holmquistite (Fig. 2A). The hornblende is intergrown with fibrous holmquistite and biotite and replaced by holmquistite along its rim. In addition to its textural relationship with hornblende, holmquistite also occurs as (1) fine-grained individual crystals, (2) sprays of fine-grained crystals, and (3) coarse-grained individual crystals. In the amphibolite surrounding the Harding pegmatite, London (1986) observed textural evidence suggesting two episodes of holmquistite formation with one

episode postdating the biotite alteration. At the Edison pegmatite site, the only textural evidence suggesting holmquistite formation postdating biotite formation is the occurrence of biotite grains being crosscut by coarse-grained holmquistite (Fig. 2A). The biotite alteration zone extends to approximately 1 m from the pegmatite contact. The textural and mineralogical characteristics of this alteration assemblage are similar to other alteration zones described by Heinrich (1965) and London (1986).

The holmquistite-hornblende alteration assemblage consists of hornblende + holmquistite + biotite (<4%) + plagioclase + quartz + ilmenite (<1%) (Figs. 2B, 2C). In assemblages with low modal abundances of holmquistite, the holmquistite occurs as small grains oriented parallel to the elongation of hornblende. In samples with high modal abundances of holmquistite, large holmquistite grains (to 0.6 cm) cut across the hornblende. In addition, holmquistite replaces hornblende along the (110) cleavage (Fig. 2B). Unlike in the biotite alteration assemblage, plagioclase is present in the mode. However, textural evidence and modal abundance suggest that the plagioclase may not be a stable phase within this assemblage. The hornblende-holmquistite alteration assemblage extends

TABLE 2. Typical chemical analyses of amphibolite adjacent to Edison pegmatite

|                                | Biotite alteration |         | Hornblende-holmquistite alteration |       |         |        | Hornblende-plagioclase |         |        |
|--------------------------------|--------------------|---------|------------------------------------|-------|---------|--------|------------------------|---------|--------|
|                                | ED1                |         | ED2                                | ED3   | ED4     | ED5    |                        | ED6     |        |
| SiO <sub>2</sub>               | 57.0               | (57.3)  | 56.7                               | 56.4  | (56.3)  | 56.2   | 53.6                   | (52.9)  | 53.0   |
| TiO <sub>2</sub>               | 1.4                | (1.4)   | 1.4                                | 1.4   | (0.6)   | 1.4    | 1.4                    | (1.6)   | 1.4    |
| Al <sub>2</sub> O <sub>3</sub> | 13.1               | (12.4)  | 12.0                               | 12.0  | (12.2)  | 12.2   | 12.0                   | (12.5)  | 12.3   |
| Fe <sub>2</sub> O <sub>3</sub> | —                  | (3.4)   | —                                  | —     | (1.6)   | —      | —                      | (1.0)   | —      |
| FeO                            | 13.7†              | (8.6)   | 15.4†                              | 16.0† | (12.6)  | 15.9†  | 15.4†                  | (12.5)  | 12.6†  |
| MnO                            | 0.1                | (0.1)   | 0.2                                | 0.2   | (0.1)   | 0.2    | 0.2                    | (0.2)   | 0.2    |
| MgO                            | 4.2                | (6.3)   | 3.8                                | 4.6   | (5.6)   | 4.1    | 4.9                    | (6.1)   | 5.8    |
| CaO                            | 5.0                | (3.7)   | 7.0                                | 7.0   | (6.7)   | 7.0    | 9.5                    | (9.3)   | 10.4   |
| Na <sub>2</sub> O              | 0.1                | (0.0)   | 1.3                                | 0.9   | (0.9)   | 1.30   | 2.5                    | (2.2)   | 2.7    |
| K <sub>2</sub> O               | 2.4                | (2.0)   | 0.4                                | 0.5   | (0.3)   | 0.6    | 0.2                    | (0.3)   | 0.8    |
| Li <sub>2</sub> O              | 1.0                | (1.1)   | 0.8                                | 0.4   | (0.3)   | 0.8    | 0.1                    | (0.0)   | 0.2    |
| F                              | 0.3                | (0.3)   | 0.1                                | 0.2   | (0.2)   | 0.2    | 0.04                   | (0.1)   | 0.04   |
| H <sub>2</sub> O*              | 2.0                | (2.6)   | 1.6                                | 1.2   | (2.0)   | 1.1    | 1.0                    | (1.3)   | 0.9    |
| S                              | —                  | (0.8)   | —                                  | —     | (0.6)   | —      | —                      | (0.0)   | —      |
| Total                          | 100.3              | (100.0) | 100.7                              | 100.8 | (100.0) | 101.00 | 100.84                 | (100.0) | 100.34 |
| As                             | 580                |         | 50                                 | 45    |         | 55     | 24                     |         | 180    |
| B                              | 224                |         | 269                                | 270   |         | 256    | 233                    |         | 158    |
| Ba                             | 250                |         | 46                                 | 85    |         | 50     | 95                     |         | 130    |
| Cs                             | 600                |         | 44                                 | 30    |         | 50     | <6                     |         | 56     |
| Cu                             | 17                 |         | 54                                 | 35    |         | 58     | 20                     |         | 9      |
| Ga                             | 18.4               |         | 20.7                               | 20.2  |         | 21.6   | 20.0                   |         | 21.4   |
| Nb                             | 12.6               |         | 11.9                               | 12.0  |         | 12.0   | 12.4                   |         | 5.0    |
| Ni                             | 64                 |         | 125                                | 50    |         | 28     | 45                     |         | 79     |
| Pb                             | 25                 |         | 14                                 | 13    |         | 21     | 14                     |         | 20     |
| Rb                             | 600                |         | 47                                 | 119   |         | 53     | 16                     |         | 66     |
| Sr                             | 125                |         | 260                                | 200   |         | 210    | 192                    |         | 180    |
| U                              | <10                |         | <7                                 | <10   |         | <10    | <5                     |         | <5     |
| Y                              | 40                 |         | 36                                 | 30    |         | 30     | 32                     |         | 17     |
| Zn                             | 164                |         | 164                                | 151   |         | 149    | 115                    |         | 82     |
| Zr                             | 166                |         | 169                                | 170   |         | 140    | 143                    |         | 78     |

Note: Whole-rock chemistries calculated from XRD-RIM modes and mineral chemistries are presented in parentheses.

\* Loss on ignition minus F content.

† Total Fe as FeO.

to approximately 5 m from the pegmatite contact. However, this distance may be deceiving because of the irregular shape of the Edison pegmatite and associated pegmatite dikes that extend beyond the wall zone of the main pegmatite body.

The hornblende-plagioclase assemblage is essentially unaltered amphibolite and consists of hornblende + plagioclase + quartz (<2%) + biotite (<2%) + ilmenite (<2%). The preferred orientation of the hornblende defines the schistosity and lineation observed in the amphibolite (Fig. 2D).

Carbonate-sulfide-arsenide veins cut across the amphibolite alteration assemblages. Amphibolite that surrounds these veins is altered to chlorite-bearing, biotite-bearing, or (carbonate + quartz)-bearing assemblages.

Typical whole-rock compositions and calculated major-element whole-rock compositions for each mineral assemblage are presented in Table 2. If normalized to relatively immobile elements such as TiO<sub>2</sub> or Al<sub>2</sub>O<sub>3</sub>, the biotite alteration assemblage is enriched (>10%) in K<sub>2</sub>O, SiO<sub>2</sub>, F, As, Pb, Ba, Cs, Li, and Rb and depleted in CaO, Na<sub>2</sub>O, and Sr relative to the hornblende-plagioclase assemblage. The major- and trace-element enrichments in this assemblage reflect the stability of biotite in the assemblage due to the metasomatic alkali-element alteration of the amphibolite and the effectiveness of biotite as a crystal-chemical trap for trace alkali elements. The

whole-rock chemistry of the hornblende-holmquistite assemblage (normalized to TiO<sub>2</sub>) appears to differ (>10%) from the unaltered hornblende-plagioclase assemblage only in Li, Cu, and Zn. The hornblende-plagioclase assemblage exhibits enrichment in alkali elements uncharacteristic of amphibolites outside the vicinity of the Harney Peak Granite and associated pegmatites. A cumulative metasomatic halo may be associated with the entire granite-pegmatite system.

## MINERAL CHEMISTRY

### Plagioclase

Plagioclase occurs in the hornblende-plagioclase and hornblende-holmquistite assemblages and is absent in the biotite alteration assemblage. Plagioclase composition in the hornblende-plagioclase amphibolite assemblage ranges from An<sub>37.3</sub>Ab<sub>62.1</sub>Or<sub>0.6</sub> to An<sub>35.2</sub>Ab<sub>64.2</sub>Or<sub>0.6</sub>. In the hornblende-holmquistite alteration assemblage, the plagioclase composition ranges from An<sub>40.0</sub>Ab<sub>59.5</sub>Or<sub>0.5</sub> to An<sub>27.5</sub>Ab<sub>72.2</sub>Or<sub>0.3</sub>. Zoning in the plagioclase in both mineral assemblages is obscure.

### Epidote

Epidote occurs only in the biotite alteration assemblage. Textural relations and chemographic interpretation indicate the epidote is a product of alteration of pla-

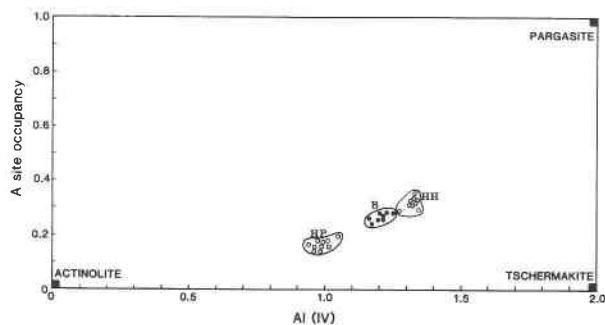


Fig. 3.  $^{IV}Al$  plotted against A-site occupancy for hornblende from the hornblende-plagioclase assemblage (HP), the hornblende-holmquistite alteration assemblage (HH), and the biotite alteration assemblage (B).

gioclase feldspar. The molecular percentage of  $Ca_2Fe_3^+Si_3O_{12}(OH)$  in the epidote ranges from 11% to 13%. The Mn component is less than 0.015 cations per formula unit.

### Biotite

Biotite is an abundant mineral phase in the biotite alteration assemblage and only an accessory phase in the hornblende-holmquistite alteration assemblage and the hornblende-plagioclase assemblage. Microprobe analyses of the biotite are given in Table 3. The  $Fe^{2+}/(Fe^{2+} + Mg)$  ratio in the biotites ranges from 0.45 to 0.48 in the hornblende-plagioclase assemblage and the hornblende-holmquistite alteration assemblage. The ratio decreases to 0.41 to 0.42 in the biotite alteration assemblage. In addition to the decrease in the  $Fe^{2+}/(Fe^{2+} + Mg)$  ratio, the biotite also exhibits a decrease in Ti and an increase in Mn, Li, and  $^{VI}Al$  from the amphibolite assemblage to the alteration assemblages. The biotite in the biotite alteration assemblage has  $Li_2O$  contents of up to 0.6 wt% and  $Fe^{3+}/(Fe^{3+} + Fe^{2+})$  ratios of 0.12 to 0.16.

### Amphiboles

The standard formula for amphiboles,  $A_{0-1}B_2^{VI}C_5^{-IV}T_8O_{22}(OH,F,Cl)_2$  (Leake, 1978), translated into site terminology reads  $A_{0-1}^{VI-VIII}(M4)_2^{VI}(M1,M2,M3)_5^{IV}T_8O_{22}^{-}(OH,F,Cl)_2$ .

Leake (1978), Hawthorne (1981, 1983), and Robinson et al. (1982) have summarized characteristics of the amphibole sites, the procedures for standard formula-unit calculation from an analysis, site assignments, and limits beyond which an analysis should be rejected.

Analyses and cation formulae for the amphiboles are given in Table 3. On the basis of the nomenclature of Leake (1978), the calcic amphiboles in the amphibolite adjacent to the Edison pegmatite may be classified as magnesio- and ferro-hornblende. Calcic amphiboles coexisting with holmquistite from southern Rhodesia (von Knorring and Hornung, 1961), southeastern Manitoba (Wright, 1963); and western Australia (Wilkins et al., 1970) are magnesio-hornblende.

The deviation of these calcic amphiboles from the

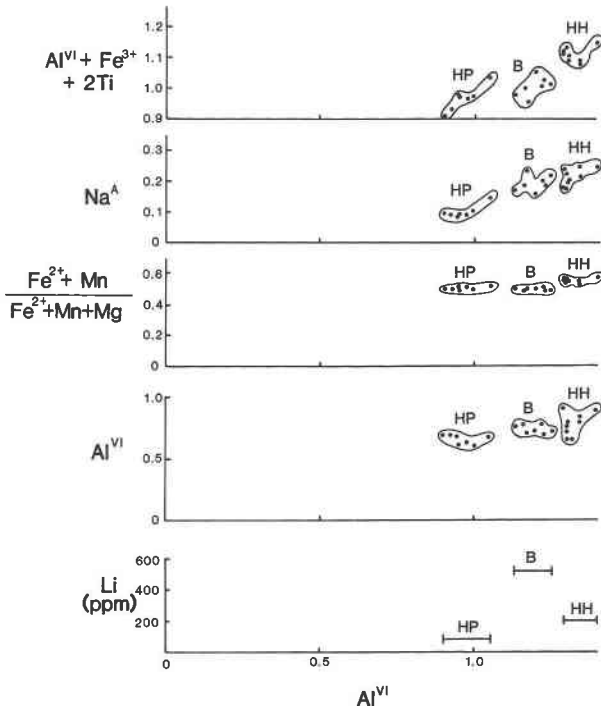


Fig. 4. Compositional characteristics of hornblende from the same assemblages as in Fig. 3.

tremolite-actinolite series ( $Ca_2(MgFe^{2+})_5Si_8O_{22}(OH)_2$ ) results from the substitution of  $Al^{3+}$  for  $Si^{4+}$  in the tetrahedral sites that is charge balanced by the substitution of trivalent (Al and  $Fe^{3+}$ ) cations for divalent cations in the octahedral sites (M1, M2, and M3) and/or by the substitution of  $Na^+$  and  $K^+$  into the A site. The deviation of the hornblende from actinolite may be partially represented in a plot of  $^{IV}Al$  against A-site occupancy (Fig. 3). The hornblende from the hornblende-holmquistite alteration assemblage deviates from actinolite more so than hornblende from either the hornblende-plagioclase or biotite assemblage. Hornblendes analyzed by von Knorring and Hornung (1961) and Wilkins et al. (1970) are further removed from the actinolite end member than those observed at the Edison pegmatite site.

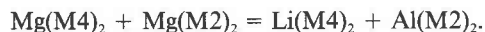
The compositional variation in the hornblende from the amphibolite and alteration zones, further illustrated in Figure 4, appears to be dependent upon associated mineral assemblages. The hornblende in the hornblende-plagioclase assemblages is typically lower in  $^{IV}Al$ ,  $^{VI}Al$ , ( $^{VI}Al + Fe^{3+} + 2Ti$ ), and Li than the hornblende from the alteration zones. The hornblende in the hornblende-holmquistite alteration zones is typically higher in  $^{IV}Al$ , ( $^{VI}Al + Fe^{3+} + 2Ti$ ), and the ratio  $(Fe^{2+} + Mn)/(Fe^{2+} + Mn + Mg)$ . Many of the compositional characteristics of the hornblende from the biotite alteration zone are intermediate or overlap with the two previously discussed assemblages with the exception of Li. The Li content of the hornblende increases in the order hornblende-plagioclase

TABLE 3A. Typical analyses of holmquistite and hornblende from amphibolite adjacent to Edison pegmatite

|                                | Holmquistite |       |       | Hornblende           |       |       |       |
|--------------------------------|--------------|-------|-------|----------------------|-------|-------|-------|
|                                | ED1A         | ED2   | ED3   | ED1A                 | ED2   | ED3   | ED5   |
| SiO <sub>2</sub>               | 59.98        | 59.95 | 59.95 | 45.21                | 44.59 | 44.73 | 47.18 |
| TiO <sub>2</sub>               | 0.07         | 0.07  | 0.03  | 0.75                 | 0.75  | 0.62  | 0.64  |
| Al <sub>2</sub> O <sub>3</sub> | 12.41        | 12.4  | 12.38 | 10.86                | 12.33 | 12.66 | 9.34  |
| Fe <sub>2</sub> O <sub>3</sub> | 4.64         | 4.43  | 4.38  | 1.28                 | 0.60  | 0.71  | 1.29  |
| FeO                            | 8.96         | 9.77  | 10.09 | 16.10                | 18.04 | 19.22 | 16.72 |
| MnO                            | 0.20         | 0.18  | 0.12  | 0.34                 | 0.34  | 0.29  | 0.27  |
| MgO                            | 7.99         | 7.57  | 7.35  | 9.07                 | 8.00  | 7.65  | 9.08  |
| CaO                            | 0.02         | 0.06  | 0.05  | 11.26                | 11.06 | 10.57 | 10.99 |
| Na <sub>2</sub> O              | 0.08         | 0.21  | 0.22  | 0.90                 | 1.04  | 1.31  | 0.92  |
| K <sub>2</sub> O               | 0.00         | 0.00  | 0.00  | 0.49                 | 0.50  | 0.38  | 0.37  |
| Li <sub>2</sub> O              | 2.92         | 2.87  | 2.95  | 0.06                 | 0.04  | 0.04  | 0.01  |
| Total                          | 97.27        | 97.51 | 97.52 | 96.32                | 97.29 | 98.18 | 96.81 |
|                                |              |       |       | Tetrahedral site     |       |       |       |
| Si                             | 7.984        | 7.988 | 7.997 | 6.801                | 6.690 | 6.670 | 7.047 |
| Al                             | 0.026        | 0.012 | 0.003 | 1.199                | 1.310 | 1.330 | 0.953 |
| T total                        | 8.000        | 8.000 | 8.000 | 8.000                | 8.000 | 8.000 | 8.000 |
|                                |              |       |       | M2 site              |       |       |       |
| Al                             | 1.921        | 1.937 | 1.942 | 0.729                | 0.872 | 0.898 | 0.693 |
| Ti                             | 0.008        | 0.008 | 0.004 | 0.086                | 0.086 | 0.072 | 0.072 |
| Fe <sup>3+</sup>               | 0.071        | 0.055 | 0.054 | 0.145                | 0.066 | 0.078 | 0.144 |
| Mg                             | 0.000        | 0.000 | 0.000 | 1.040                | 0.976 | 0.952 | 1.091 |
| M2 Total                       | 2.000        | 2.000 | 2.000 | 2.000                | 2.000 | 2.000 | 2.000 |
|                                |              |       |       | M1, M2, and M3 sites |       |       |       |
| Fe <sup>3+</sup>               | 0.393        | 0.388 | 0.384 | —                    | —     | —     | —     |
| Mg                             | 1.584        | 1.506 | 1.459 | 0.993                | 0.809 | 0.750 | 0.929 |
| Fe                             | 1.000        | 1.089 | 1.122 | 2.007                | 2.191 | 2.250 | 2.071 |
| Mn                             | 0.023        | 0.017 | 0.016 | 0.000                | 0.000 | 0.000 | 0.000 |
| Ca                             | 0.000        | 0.000 | 0.008 | 0.000                | 0.000 | 0.000 | 0.000 |
| M1-M3 total                    | 3.000        | 3.000 | 2.989 | 3.000                | 3.000 | 3.000 | 3.000 |
|                                |              |       |       | M4 site              |       |       |       |
| Fe                             | 0.000        | 0.000 | 0.000 | 0.026                | 0.072 | 0.151 | 0.021 |
| Mn                             | 0.001        | 0.007 | 0.000 | 0.045                | 0.045 | 0.036 | 0.036 |
| Ca                             | 0.000        | 0.008 | 0.000 | 1.817                | 1.776 | 1.685 | 1.760 |
| Li                             | 1.568        | 1.538 | 1.587 | 0.036                | 0.018 | 0.018 | 0.000 |
| Na                             | 0.016        | 0.048 | 0.048 | 0.076                | 0.089 | 0.011 | 0.183 |
| M4 total                       | 1.585        | 1.601 | 1.635 | 2.000                | 2.000 | 2.000 | 2.000 |
|                                |              |       |       | A site               |       |       |       |
| Na                             | 0.000        | 0.000 | 0.000 | 0.195                | 0.218 | 0.266 | 0.086 |
| K                              | 0.000        | 0.000 | 0.000 | 0.090                | 0.090 | 0.072 | 0.072 |
| A total                        | 0.000        | 0.000 | 0.000 | 0.285                | 0.308 | 0.338 | 0.158 |

assemblage, hornblende-holmquistite alteration assemblage, biotite-alteration assemblage.

Holmquistite is a Li-rich, Fe-Mg-Mn amphibole (Hawthorne, 1981, 1983) with an ideal formula of  $\text{Li}_2\text{Al}_2(\text{Mg}, \text{Fe}^{2+})_3\text{Si}_4\text{O}_{22}(\text{OH})$ . It is isostructural with the anthophyllite-gedrite series and chemical differences between the two amphiboles are primarily a function of the exchange component



Refinement of the orthorhombic holmquistite structure (Whittaker, 1969; Litvin et al., 1973; Finger and Ohashi 1974a, 1974b; Law, 1973; Irusteta and Whittaker, 1975) and infrared absorption data (Wilkins et al., 1970) has confirmed a *Pnma* space group and has constrained site occupancy models. Rationale behind site assignments in Table 3 is based on these models. Ginsburg (1965) has also identified monoclinic holmquistite.

The holmquistite in the amphibolite adjacent to the Edison pegmatite occurs only in the alteration assem-

blages associated with the pegmatite fluid-amphibolite interaction. The holmquistite in these alteration zones has the tetrahedral sites essentially filled with Si (= 8.000), Li in M4 ranges from 1.538 to 1.587, Al<sup>3+</sup> in M2 ranges from 1.921 to 1.942 and (Al<sup>3+</sup> + Fe<sup>3+</sup> + 2Ti) ranges from 2.363 to 2.408 cations per formula unit. The analyses also indicate that the M4 site of the holmquistite from this location is only partially filled by Li. Low Li concentrations in holmquistite resulting in low M4-site occupancy have been previously reported (e.g., Karpoff, 1960). This low M4-site occupancy may be the result of Li loss during weathering of holmquistite. In addition, weathering or alteration of spodumene can result in Li loss and low M2-site (in spodumene) occupancy (Roberts and Rapp, 1965). The ratio Fe<sup>2+</sup>/(Fe<sup>2+</sup> + Mg) in the holmquistite decreases from the hornblende-holmquistite alteration zone (0.43) to the biotite alteration zone (0.38). Holmquistite from the biotite alteration zone (sample ED1A) has the following unit-cell parameters:  $a = 18.254 \pm 0.005$ ,  $b = 17.621 \pm 0.009$ , and  $c = 5.295 \pm 0.003$ .

TABLE 3B. Typical analyses of biotite from amphibolite adjacent to Edison pegmatite

|                                | ED1A* | ED2   | ED5   |
|--------------------------------|-------|-------|-------|
| SiO <sub>2</sub>               | 37.06 | 36.36 | 36.60 |
| TiO <sub>2</sub>               | 0.94  | 1.02  | 2.86  |
| Al <sub>2</sub> O <sub>3</sub> | 17.06 | 18.46 | 16.32 |
| Fe <sub>2</sub> O <sub>3</sub> | 4.80  | 4.45  | 4.86  |
| FeO                            | 13.50 | 14.50 | 15.00 |
| MnO                            | 0.12  | 0.26  | 0.11  |
| MgO                            | 10.83 | 9.78  | 9.41  |
| CaO                            | 0.13  | 0.09  | 0.02  |
| Na <sub>2</sub> O              | 0.01  | 0.00  | 0.08  |
| K <sub>2</sub> O               | 10.11 | 10.20 | 10.32 |
| Li <sub>2</sub> O              | 0.60  | n.d.  | n.d.  |
| Total                          | 95.16 | 95.12 | 95.58 |
| Tetrahedral site               |       |       |       |
| Si                             | 5.568 | 5.496 | 5.500 |
| Al                             | 2.432 | 2.504 | 2.500 |
| T Total                        | 8.000 | 8.000 | 8.000 |
| Octahedral site                |       |       |       |
| Al                             | 0.608 | 0.784 | 0.414 |
| Ti                             | 0.108 | 0.118 | 0.328 |
| Fe <sup>3+</sup>               | 0.542 | 0.508 | 0.552 |
| Mg                             | 2.426 | 2.206 | 2.122 |
| Fe <sup>2+</sup>               | 1.696 | 1.834 | 1.904 |
| Mn                             | 0.018 | 0.036 | 0.018 |
| Li                             | 0.360 | —     | —     |
| Oct. total                     | 5.758 | 5.486 | 5.338 |
| Interlayer site                |       |       |       |
| Ca                             | 0.018 | 0.018 | 0.000 |
| Na                             | 0.000 | 0.000 | 0.018 |
| K                              | 1.932 | 1.962 | 2.002 |
| Total                          | 1.944 | 1.980 | 2.020 |

\* F = 0.60%, H<sub>2</sub>O = 3.85%, X<sub>Mg</sub> = 0.421, X<sub>Ann</sub> = 0.295, X<sub>Sid</sub> = 0.106, log X<sub>F</sub>/X<sub>OH</sub> = 1.13, IV(F)<sub>bo</sub> = 1.92.

## DISCUSSION

### Hornblende-holmquistite relations

The crystal-chemical relationships between actinolite-hornblende series clin amphiboles and anthophyllite-gedrite series orthoamphiboles have been documented in numerous studies (summarized by Robinson et al., 1982). Ross et al. (1968, 1969), Papike et al. (1969), and Robinson et al. (1982) emphasized the importance of the M4-site occupancy on the structural type and phase relations of the calcic and Fe-Mg amphiboles. The discontinuity in size between cations in the M4 site is the major crystal-chemical control on the calcic amphibole and Fe-Mg amphibole miscibility gap. Insight into the crystal-chemical behavior and phase relationships between coexisting holmquistite-calcic amphibole pairs may be gained by analogy to the better understood calcic amphibole-FeMg amphibole pairs. Such an analogy appears to be appropriate as holmquistite is isostructural with anthophyllite-gedrite series orthoamphiboles and the M4-site cations are similar in size with Li<sup>+</sup> (0.68 Å) being intermediate in size between Mg<sup>2+</sup> (0.66 Å) and Fe<sup>2+</sup> (0.74 Å) (Ahrens, 1952). If analogous to the relationship between calcic and Mg-Fe amphiboles, the difference in M4-site cation size and charge between Ca and Li in coexisting hornblende-holmquistite may result in a large miscibility gap. Unlike the phase and structural relationships in the calcic and Mg-Fe amphiboles, a monoclinic Li amphibole (clino-

holmquistite) analogous to cummingtonite-grunerite has been observed in only a few locations and appears to be far subordinate to orthorhombic holmquistite in Li-Ca amphibole assemblages. This difference between calcic and Mg-Fe amphiboles and Li-Ca amphiboles may be due to the limited temperature range of Li metasomatism adjacent to pegmatites (London, 1986), bulk-rock compositions resulting from the metasomatic extraction of Ca from the metasomatized amphibolite, and complications in analogous phase relationships resulting from the occurrence of Al in the M2 site in holmquistite and Mg-Fe in the M2 site in Mg-Fe amphibole anthophyllite.

The compositional variability between coexisting holmquistite and hornblende from the amphibolite adjacent to the Edison pegmatite is shown in Figure 5. The miscibility gap is extremely wide, with the holmquistite having Ca/(Ca + Na + Li) less than 0.01 and the Ca/(Ca + Li) ratio of the hornblende greater than 0.99. This wide gap appears to be typical, but exceptions have been documented (Heinrich, 1965). The high R<sup>3+</sup> (octahedral Al + Fe<sup>3+</sup> + 2Ti<sup>4+</sup>) value for the holmquistite relative to the coexisting hornblende contrasts with coexisting calcic amphibole-orthorhombic amphibole pairs in which the calcic amphibole contains a higher proportion of R<sup>3+</sup> substitution (Robinson et al., 1982). In addition, there is a marked preference for Fe<sup>3+</sup> in holmquistite relative to hornblende.

As shown in Figure 5B, the ratio of (Fe<sup>2+</sup> + Mn)/(Fe<sup>2+</sup> + Mn + Mg) for the coexisting Li-rich and calcic amphiboles is slightly greater in the hornblende relative to the holmquistite. In most of calcic and Mg-Fe orthoamphibole pairs, the calcic amphibole shows a slight depletion of Fe<sup>2+</sup> relative to the coexisting amphibole (Robinson et al., 1982).

### Alteration of the amphibolite

The alteration of the amphibolite adjacent to the Edison pegmatite appears to be the result of (1) Li and K metasomatic alteration by alkali-rich, pegmatite-derived aqueous fluids and (2) retrograde metamorphism of the amphibolite by the aqueous fluids resulting in the instability of plagioclase and ilmenite and the formation of epidote and sphene.

Differences in modal and chemical compositions between the unaltered amphibolite and the two alteration zones may be helpful in illustrating the nature of the metasomatic chemical reactions and the behavior of mobile species within the alteration zone (Shearer et al., 1984). Sample ED5 from the unaltered amphibolite assemblage is compared to both sample ED3, from the hornblende-holmquistite alteration assemblage, and sample ED1, from the biotite alteration assemblage, to compare the chemical and modal differences between the assemblages and to approximate reactions occurring within the alteration zones. Bulk compositions from both the RIM-XRD modal data and the microprobe data have been used for mass-balance calculations to evaluate sample homogeneity, to estimate unanalyzed components



TABLE 4. Mass balance between altered and unaltered amphibolite assemblages

|          | Mineral balance* |        |        |        |        |        |        |        |        |        |
|----------|------------------|--------|--------|--------|--------|--------|--------|--------|--------|--------|
|          | Qtz              | Pl     | Hbl    | Bt     | Holm   | Ep     | Chl    | Ilm    | Py     | Spn    |
| ED5      | 7.0              | 23.2   | 67.3   | 0.1    | 0.0    | 0.0    | 0.0    | 2.4    | 0.0    | 0.0    |
| ED1      | 20.0             | 0.0    | 6.0    | 20.0   | 35.8   | 9.1    | 4.4    | 0.0    | 1.5    | 3.2    |
| Net      | +13.0            | -23.2  | -61.3  | +19.9  | +35.8  | +9.1   | +4.4   | -2.4   | +1.5   | +3.2   |
| <i>M</i> | +0.216           | -0.096 | -0.068 | +0.022 | +0.048 | +0.020 | +0.004 | -0.016 | +0.013 | +0.016 |
| <i>V</i> | +4.9             | -8.7   | -18.9  | +6.6   | +11.5  | +2.7   | +1.5   | -0.5   | +0.3   | +0.9   |
| ED5      | 7.0              | 23.2   | 67.3   | 0.1    | 0.0    | 0.0    | 0.0    | 2.4    | 0.0    | 0.0    |
| ED3      | 16.9             | 4.2    | 47.3   | 0.4    | 18.6   | 6.5    | 4.4    | 0.5    | 1.1    | 0.0    |
| Net      | +9.9             | -19.0  | -20.0  | +0.3   | +18.6  | +6.5   | +4.4   | -1.9   | +1.1   | 0.0    |
| <i>M</i> | +0.165           | -0.071 | -0.022 | 0.000  | +0.025 | +0.014 | +0.004 | -0.013 | +0.009 | 0.000  |
| <i>V</i> | +3.7             | -7.1   | -6.2   | +0.1   | +6.0   | +1.9   | +1.5   | -0.4   | +0.2   | 0.0    |

|          | Chemical balance |                  |                                |                                |        |        |        |        |                   |                  |
|----------|------------------|------------------|--------------------------------|--------------------------------|--------|--------|--------|--------|-------------------|------------------|
|          | SiO <sub>2</sub> | TiO <sub>2</sub> | Al <sub>2</sub> O <sub>3</sub> | Fe <sub>2</sub> O <sub>3</sub> | FeO    | MnO    | MgO    | CaO    | Na <sub>2</sub> O | K <sub>2</sub> O |
| ED5      | 52.9             | 1.6              | 12.5                           | 1.0                            | 12.5   | 0.2    | 6.1    | 9.3    | 2.2               | 0.3              |
| ED1      | 57.3             | 1.4              | 12.4                           | 3.4                            | 8.6    | 0.1    | 6.3    | 3.7    | 0.0               | 2.0              |
| Net      | +4.4             | -0.2             | -0.1                           | +2.4                           | -3.9   | -0.1   | +0.2   | -5.6   | -2.2              | +1.7             |
| <i>M</i> | +0.073           | -0.003           | 0.000                          | +0.015                         | -0.054 | 0.001  | 0.005  | -0.099 | -0.036            | +0.018           |
| ED5      | 52.9             | 1.6              | 12.5                           | 1.0                            | 12.5   | 0.2    | 6.1    | 9.3    | 2.2               | 0.3              |
| ED3      | 56.3             | 0.6              | 12.2                           | 1.6                            | 12.6   | 0.1    | 5.6    | 6.7    | 0.9               | 0.3              |
| Net      | +3.4             | -1.0             | -0.3                           | +1.6                           | +0.1   | -0.1   | -0.5   | -2.6   | -1.3              | 0.0              |
| <i>M</i> | +0.057           | -0.013           | -0.003                         | +0.010                         | -0.001 | -0.001 | -0.012 | -0.046 | -0.021            | 0.000            |

Note: Modes or oxides normalized to 100 g. Net = weight difference (in grams) between samples. *M* = Net divided by formula weight. *V* = Net divided by volume.  
 \* Abbreviations: Qtz = quartz, Pl = plagioclase, Hbl = hornblende, Bt = biotite, Holm = holmquistite, Ep = epidote, Chl = chlorite, Ilm = ilmenite.

(H<sub>2</sub>O), and to establish closure between the modal and chemical data sets. The weight percent H<sub>2</sub>O was calculated on the basis of mineral stoichiometry (hornblende, holmquistite, biotite) and loss on ignition.

Using the calculated chemical analyses standardized to 100% for the unaltered amphibolite and the two alteration assemblages, mass-balance calculations for mineral and chemical exchange and volume loss are presented in

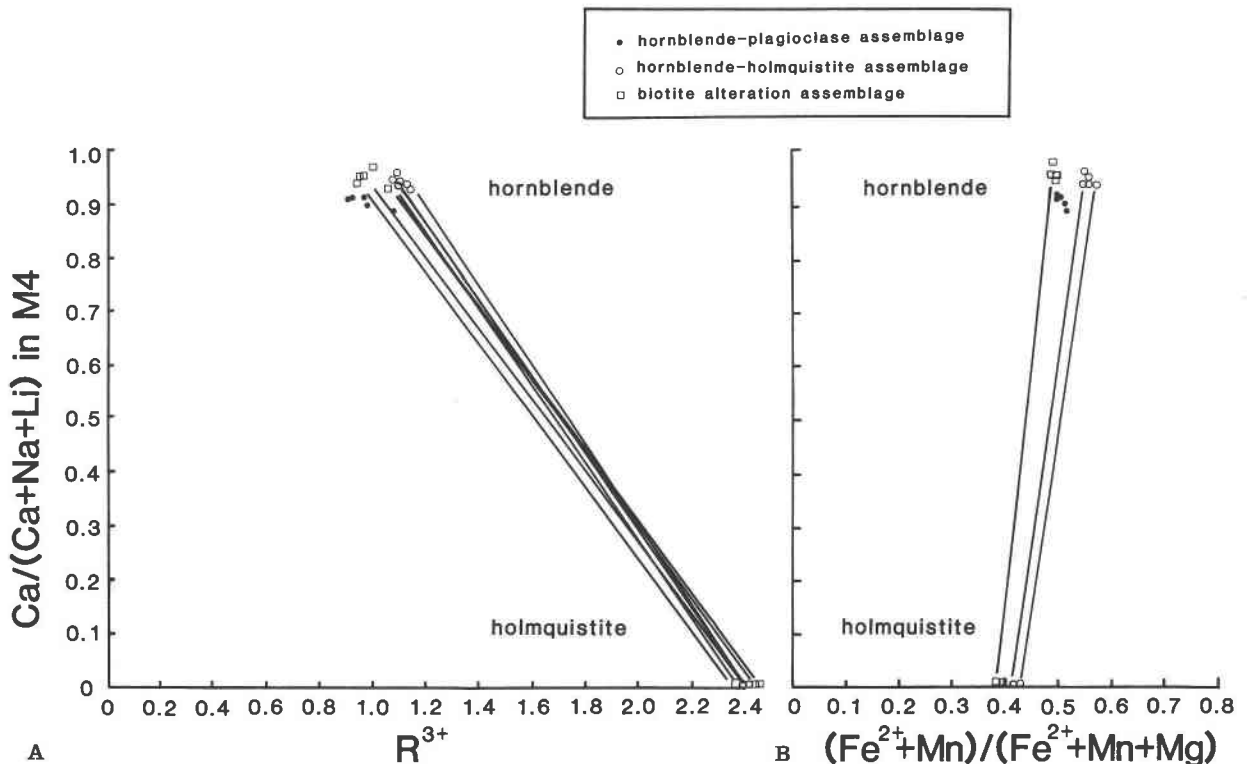


Fig. 5. Comparison of coexisting calcic amphiboles and Li-rich amphiboles in the amphibolite adjacent to the Edison pegmatite. (A) Plot of Ca/(Ca + Na + Li) in M4 vs. R<sup>3+</sup> (octahedral Al + Fe<sup>3+</sup> + 2Ti<sup>4+</sup>). (B) Plot of Ca/(Ca + Na + Li) in M4 vs. (Fe<sup>2+</sup> + Mn)/(Fe<sup>2+</sup> + Mn + Mg).

TABLE 4—Continued

| Mineral balance*         |        |                  |        |
|--------------------------|--------|------------------|--------|
| $\Delta_{\text{solids}}$ |        |                  |        |
| +0.3                     |        |                  |        |
| -0.3                     |        |                  |        |
| Chemical balance         |        |                  |        |
| Li <sub>2</sub> O        | F      | H <sub>2</sub> O | S      |
| 0.0                      | 0.1    | 1.3              | 0.0    |
| 1.1                      | 0.3    | 2.6              | 0.8    |
| +1.1                     | +0.2   | +1.3             | +0.8   |
| +0.037                   | +0.011 | +0.072           | +0.025 |
| 0.0                      | 0.1    | 1.3              | 0.0    |
| 0.6                      | 0.2    | 2.0              | 0.6    |
| +0.6                     | +0.1   | +0.7             | +0.6   |
| +0.020                   | 0.005  | +0.039           | +0.019 |

by  $\rho$ .

Py = pyrite, Spn = sphene.

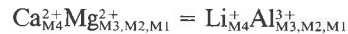
Table 4. Mineral exchange between assemblages (Table 4) indicates substantial decrease in plagioclase, hornblende, and ilmenite with alteration and replacement by holmquistite, quartz, biotite (ED1), and epidote. Assemblage volume calculations and limited variability of non-mobile elements (Al, Ti, Nb) indicate volume was conserved during alteration.

Differences between ED5 and ED3 indicate the mineral differences may be a result of the addition of Li<sub>2</sub>O (0.6 g/100 g), SiO<sub>2</sub> (3.4 g/100 g), and S (0.6 g/100 g) and the removal of Na<sup>+</sup> (1.3 g/100 g) and Ca<sup>2+</sup> (2.6 g/100 g) from the amphibolite. The biotite assemblage, however, shows a much more striking contrast in chemistry compared to the unaltered amphibolite. Li<sub>2</sub>O (1.1 g/100 g), SiO<sub>2</sub> (4.4 g/100 g), S (0.8 g/100 g), K<sub>2</sub>O (1.7 g/100 g), F (0.2 g/100 g), and H<sub>2</sub>O (1.3 g/100 g) are apparently added to the system, whereas Ca<sup>2+</sup> (5.6 g/100 g) and Na<sup>+</sup> (2.2 g/100 g) are removed. Losses and gains of Fe<sub>2</sub>O<sub>3</sub> and FeO appear to offset one another in a comparison of ED5 and ED1, suggesting oxidation of the biotite assemblage.

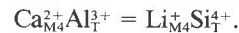
The calculations identify mobile components added to the system (Li<sup>+</sup>, K<sup>+</sup>, Si<sup>4+</sup>, H<sub>2</sub>O), those removed from the system (Ca<sup>2+</sup>, Na<sup>+</sup>), and possible reactions involving the consumption of feldspar, hornblende, and ilmenite and the production of biotite, holmquistite, and epidote. The mobile components and possible reactions indicated by these exchange calculations contrast markedly with the metasomatic alteration of schist adjacent to many Black Hills pegmatites (Shearer et al., 1984). In the schist adjacent to the Tip Top pegmatite, B<sup>3+</sup>, Na<sup>+</sup>, Fe, and Li were preferentially added to the system by pegmatite-derived fluids, whereas K, Mg, and Si were removed from the schist. This resulted in the stability of tourmaline at the expense of biotite. Differences in alteration-mineral assemblages obviously reflect original country-rock char-

acteristics but also reflect differences in pegmatite-fluid composition (Shearer et al., 1986).

Numerous chemographic representations have been used to illustrate phase relations and reactions in amphibole-bearing assemblages and metasomatically altered amphibolites (e.g., Robinson et al., 1982; London, 1986). The metasomatic alteration of amphibolite adjacent to the Edison pegmatite may be approximately represented graphically in a A-C-Li<sub>2</sub>O-K<sub>2</sub>O tetrahedron where C = (CaO + FeO + MnO + MgO - TiO<sub>2</sub>) and A = (Al<sub>2</sub>O<sub>3</sub> + Fe<sub>2</sub>O<sub>3</sub> + TiO<sub>2</sub> - Na<sub>2</sub>O) (Fig. 6). The original amphibolite bulk composition (BC1) plots on the hornblende-plagioclase-biotite plane near the hornblende-plagioclase tie line. With the addition of substantial amounts of Li, the bulk composition (BC2) moves into the hornblende-holmquistite-plagioclase-biotite volume. The reaction resulting in the appearance of holmquistite in these amphibolites suggested by the mass balance in Table 4 and the chemography may be represented by Reaction 1 in Table 5. Na<sup>+</sup> and Ca<sup>2+</sup> are either transported out of the system (calcite-sulfide-arsenide veins) or are involved in formation of additional epidote (Ca), sphene (Ca), and retrograde exchange reactions NaSiCa<sub>-1</sub>Al<sub>-1</sub> in plagioclase. The principal exchange reactions occurring between the hornblende and holmquistite are



and



The formation of the biotite alteration zone (BC3) requires the addition of K<sup>+</sup> and perhaps additional Li to BC2 (Fig. 6). Based on textural evidence, biotite is not formed at the expense of holmquistite but rather through the breakdown of hornblende. A reaction calculated from Table 4 and using the chemography may be represented by Reaction 2 in Table 5. K<sub>fluid</sub><sup>+</sup> and S<sub>fluid</sub> are derived from the pegmatite fluid. The epidote and sphene accessory minerals of the biotite alteration zone are typical of mineral assemblages associated with greenschist-facies conditions. Retrograde-type reactions involved in the breakdown of plagioclase and the stabilization of epidote and sphene in mafic igneous rocks have been discussed in great detail (e.g., Robinson et al., 1982).

The spatial relations of the metasomatic mineral assemblages indicate that the K<sup>+</sup>/Li<sup>+</sup> ratio in the pegmatite-derived fluid was highest during the initial fluid-amphibolite interaction at the pegmatite contact (biotite alteration zone; K<sup>+</sup>/Li<sup>+</sup> = 0.45) and subsequently decreased with distance from the pegmatite contact (hornblende-holmquistite alteration zone; K<sup>+</sup>/Li<sup>+</sup> < 0.1). Several scenarios of fluid-amphibolite interaction are suggested: (1) a single episode of fluid-amphibolite interaction. The high "relative reactivity" of K<sup>+</sup> and higher "relative mobility" of Li<sup>+</sup> (Shearer et al., 1986; cf. Kharaka and Berry, 1973) resulted in depletion of K<sup>+</sup> in the fluid relative to Li<sup>+</sup>. This depletion is manifested in the biotite alteration zone occurring at the pegmatite contact; and (2) two episodes of fluid-amphibolite interaction with either individual K<sup>+</sup>-

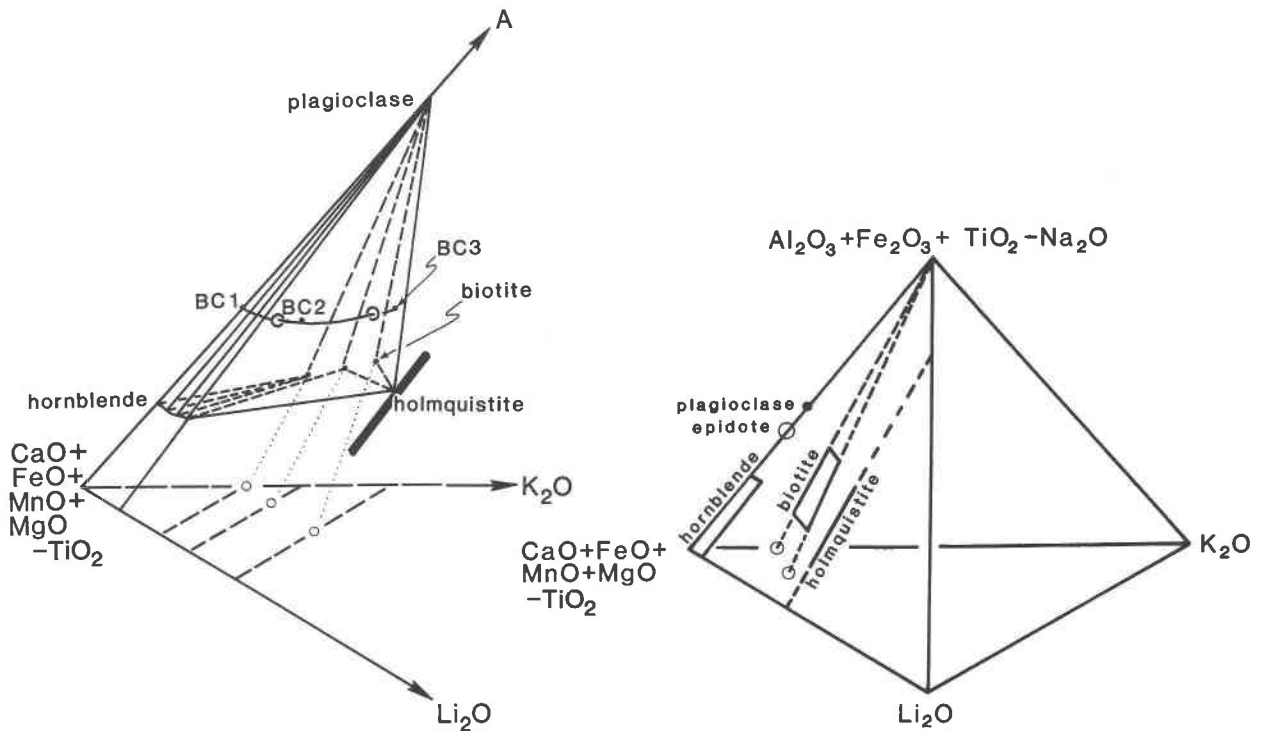


Fig. 6. Amphibolite and alteration assemblages adjacent to the Edison pegmatite depicted in an A-C-Li<sub>2</sub>O-K<sub>2</sub>O tetrahedron where C = (CaO + FeO + MnO + MgO - TiO<sub>2</sub>) and A = (Al<sub>2</sub>O<sub>3</sub> + Fe<sub>2</sub>O<sub>3</sub> + TiO<sub>2</sub> - Na<sub>2</sub>O). Biotite compositions are projected from A apex onto the C-Li<sub>2</sub>O-K<sub>2</sub>O plane. With the retrograde alteration of plagioclase, tie lines will extend to epidote rather than plagioclase.

rich fluid and Li<sup>+</sup>-rich fluid or a continuous interaction of evolving pegmatite fluids (k<sup>+</sup>-rich to Li<sup>+</sup>-rich). Although not definitive, textural evidence suggests that the K metasomatic episode preceded the Li metasomatic episode. Biotite only replaces hornblende, whereas holmquistite replaces hornblende and cuts across biotite grains. Discrimination between the single fluid-amphibolite interaction model and the multiple fluid-amphibolite interaction model is inconclusive at the Edison pegmatite. A separate late-stage Li-metasomatism episode has been documented at other pegmatites (London, 1986).

Assuming a single episode of fluid-country rock interaction, alkali-element concentrations in the pegmatite-derived fluid phase have been estimated by Shearer et al. (1986) and Walker (1984) using the relationship, defined by Nabelek (1987),

$$C_s^f = C_s^i D - e^{-N/D}(C_s^i D - C_s^i),$$

where  $C_s^f$  is the final concentration of the trace element in the enriched rock,  $C_s^i$  is the initial concentration of the trace element in the fluid,  $D$  is the rock/fluid bulk distribution coefficient calculated from the mineral/fluid distribution coefficients (Walker, 1984; Volfinger and Robert, 1980) for similar amphibolite assemblages (e.g., Walker, 1984),  $N$  is an equivalent mass of fluid relative to the rock, and  $C_s^i$  is the initial concentration of a trace element in the rock prior to fluid enrichment.

Assuming an unaltered rock composition of Li = 70 ppm and Rb = 10 ppm (Walker, 1984) and a series of hypothetical initial fluid compositions ( $C_f$ ), rock-enrichment curves may be constructed from the trace-element equation. On the basis of the fluid-composition construction (Fig. 7), the Rb/Li ratio in the pegmatite-derived fluid decreased from the amphibolite immediately adjacent to the pegmatite (biotite alteration assemblage) to the amphibolite farther away from the pegmatite contact (hornblende-holmquistite alteration assemblage and hornblende-plagioclase assemblage). This is in agreement with the high K content of the fluid implied by the biotite alteration assemblage. The results in Figure 7 are non-unique; however, minimum alkali concentrations may be calculated. By making  $N$  very large, Equation 1 is reduced to

$$C_s^f = C_s^i D,$$

where  $C_f$  is equal to the minimum alkali-element concentration in the fluid (Walker, 1984). By this method the approximate minimum concentration of the alkali elements in the initial fluid phase (biotite alteration assemblage) at the Edison pegmatite was calculated as Rb = 2730 and Li = 1600. The much lower fluid/rock ratios implied by other pegmatite studies (Walker, 1984; London, 1986; Shearer et al., 1986) and metamorphic-fluid studies (Ferry, 1978) suggest that the Rb and Li concen-

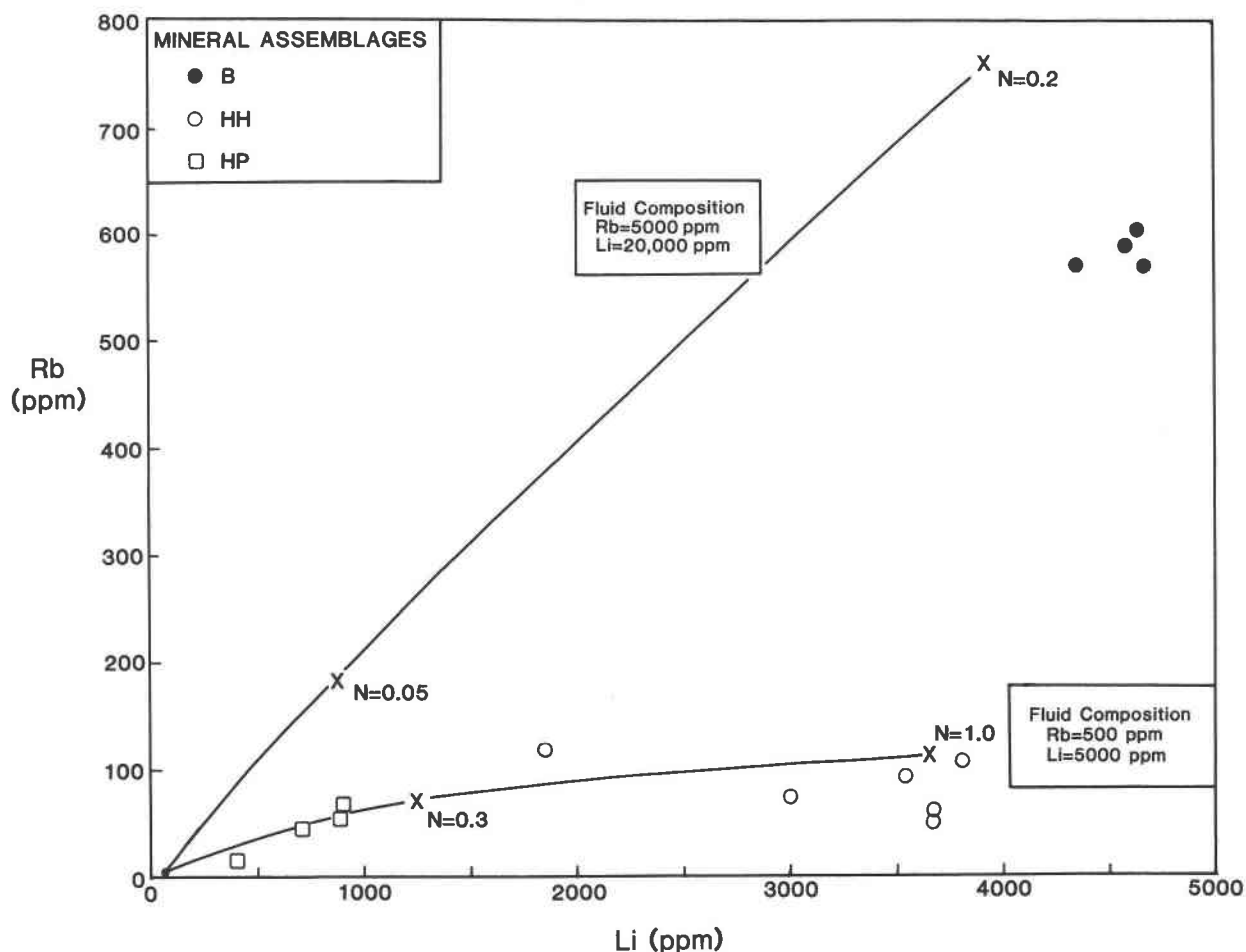


Fig. 7. Modeling of fluid-rock interaction in amphibolite with Li- and Rb-bearing fluids with series of hypothetical fluid compositions. Curves indicate the compositional paths of the amphibolite equilibrating with infiltrating fluids of different compositions. The Xs represent various values of  $N$ , the ratio of mass of fluid to rock.

trations of the fluids are much higher than these minimum estimates.

Calculation of  $\log(f_{\text{H}_2\text{O}}/f_{\text{HF}})$  for the aqueous solutions may be made using the experimental calibration of F-OH exchange between biotite and fluid made by Munoz and Ludington (1974) and Munoz (1984). It has been documented, however, that substantial Li substitution into biotite may have a strong effect on the partitioning of F into biotite (Munoz, 1984). The calculated F intercept values for Li-enriched biotite are likely to be depressed (Munoz, 1984), but still may be compared to biotites of

similar Li content to determine relative  $\log(f_{\text{H}_2\text{O}}/f_{\text{HF}})$  of pegmatite-derived aqueous solutions. The calculated  $\log(f_{\text{H}_2\text{O}}/f_{\text{HF}})$  for the fluid interacting with amphibolite adjacent to the Edison pegmatite is 4.60 at 530 °C and 3.35 at 365 °C (Table 3). Compared to biotites with similar Li content, the  $\log(f_{\text{H}_2\text{O}}/f_{\text{HF}})$  value for the fluid at the Edison pegmatite is similar to calculated  $\log(f_{\text{H}_2\text{O}}/f_{\text{HF}})$  values from other spodumene-bearing pegmatites in the Black Hills and higher than lepidolite-bearing pegmatites in the Black Hills (Shearer et al., 1986). The relationship between the fugacity of HF and lithium aluminosilicate stability has

TABLE 5. Possible reactions that approximate observed chemical and mineral variations in amphibolite

| Reaction 1   |  |
|--|--|
| $1\text{PI} + 0.31\text{Hbl} + 0.18\text{Ilm} + 0.25\text{S} + 0.56\text{Li}^+ + 1.25\text{Si} + 0.16\text{F} + 1.01\text{H}_2\text{O} = 2.32\text{Qtz} + 0.35\text{Holm} + 0.20\text{Ep} + 0.06\text{Chl} + 0.13\text{Py} + 0.69\text{Na}^+ + 0.94\text{Ca}^{2+}$   |  |
| Reaction 2   |  |
| $1.0\text{PI} + 0.79\text{Hbl} + 0.19\text{Ilm} + 0.44\text{K}^+ + 0.97\text{Li}^+ + 0.30\text{S} + 0.13\text{F} + 1.36\text{Si} + 0.34\text{Fe}^{3+} + 0.84\text{H}_2\text{O} = 2.51\text{Qtz} + 0.26\text{Bt} + 0.56\text{Holm} + 0.23\text{Ep} + 0.05\text{Chl} + 0.15\text{Py} + 0.19\text{Spn} + 1.14\text{Ca}^{2+} + 0.80\text{Na}^+ + 0.42\text{Fe}^{2+}$ |  |

Note: Derived from mass-balance data in Table 4. Abbreviations of minerals listed in Table 4.

been discussed by London (1982), Černý and Burt (1984) and Shearer et al. (1986).

The *P* and *T* conditions under which the holmquistite-bearing assemblage adjacent to the Edison pegmatite formed can at best be only approximated. The country rock in the immediate vicinity of the Edison pegmatite was metamorphosed to staurolite grade. Peak metamorphic conditions of *T* = 565 °C (Willibey, 1975) and *P* = 3–4 kbar (Redden et al., 1982) set an upper limit to conditions of holmquistite assemblage formation. Retrograde mineral assemblages, particularly in the biotite alteration zone, suggest that alteration zone formation may have occurred at temperatures well below 565 °C. Retrograde metamorphic temperatures of 510 °C (garnet core) to 365 °C (garnet rim) have been estimated for metasomatic alteration zones in schist adjacent to other Black Hills pegmatites (unpub. data of authors). These temperatures are based upon the Mg-Fe exchange between coexisting garnet and biotite. The temperature calculated from garnet rim–biotite pairs are probably the most reasonable temperatures for the formation of holmquistite assemblages. Conditions at which holmquistite assemblages are stable have been discussed by London (1986). He concluded that holmquistite assemblages adjacent to pegmatites represent greenschist-facies conditions and that holmquistite may be stable down to 350 °C.

### CONCLUSIONS

Several conclusions can be reached concerning the interaction between Edison pegmatite-derived fluids and adjacent amphibolites. Obviously, the fluids derived from the Edison pegmatite were enriched in K<sup>+</sup> and Li<sup>+</sup>. The absence of tourmaline in the altered country rock suggests that B was in low concentration in the fluid or was coordinated in the fluid in a manner to decrease its reactivity with the country rock. This appears to be typical of many of the highly evolved pegmatites in the Black Hills. These fluids interacted with amphibolite resulting in the formation of three distinct mineral assemblages: (1) biotite alteration assemblage (biotite + holmquistite ± hornblende ± plagioclase + quartz + sphene + epidote); (2) hornblende-holmquistite alteration assemblage (hornblende + holmquistite + plagioclase + quartz ± ilmenite ± biotite); and (3) hornblende-plagioclase assemblage (hornblende + plagioclase ± quartz ± biotite). These assemblages are primarily the result of (1) reactions between hornblende and aqueous fluids enriched in K<sup>+</sup> and Li<sup>+</sup> and (2) retrograde re-equilibration of plagioclase, ilmenite, and biotite with the aqueous fluid. The conditions at which the alteration occurred were below 565 °C and 3–4 kbar and probably closer to 365 °C and 3–4 kbar. Field and textural evidence cannot discriminate between a single fluid–amphibolite interaction model and a multiple fluid–amphibolite interaction model. If a multiple-fluid or evolving interaction model is correct, the K<sup>+</sup>-enriched fluids interacted with the amphibolite prior to the Li-enriched fluids.

### ACKNOWLEDGMENTS

This research was supported by the U.S. Department of Energy under Grant DE-FG01-84ER-13259. We thank J. J. Norton and J. A. Redden for their advice concerning holmquistite mineral assemblages in the Black Hills, David London for his input during the beginning of this project, and J. C. Laul for providing xrf analyses of selected samples. John Schumacher, David London, and George Morgan provided additional and valuable insight to this problem through their thorough review of this manuscript.

### REFERENCES CITED

- Ahrens, L.H. (1952) The use of ionization potentials. *Geochimica et Cosmochimica Acta*, 16, 155–169.
- Bence, A.E., and Albee, A.L. (1968) Empirical correction factors for the electron microanalysis of silicates and oxides. *Journal of Geology*, 76, 382–403.
- Beus, A.A. (1960) Geochemistry of beryllium and genetic types of beryllium deposits. Academy of Science USSR Moscow (in Russian) (translation, Freeman & Co., San Francisco, 1966, 329 p.).
- Černý, P. (1982) Petrogenesis of granite pegmatites. *Mineralogical Association of Canada short course Handbook*, 8, 405–461.
- Černý, P., and Burt, D.M. (1984) Paragenesis, crystallochemical characteristics and geochemical evolution of micas in granitic pegmatites. *Mineralogical Society of America Reviews in Mineralogy*, 13, 257–297.
- Davis, B.L. (1978) Additional suggestions for X-ray quantitative analysis of high-volume filters. *Atmospheric Environment*, 12, 2403–2406.
- (1980) "Standardless" X-ray diffraction quantitative analysis. *Atmospheric Environment*, 14, 217–220.
- Ferry, J.M. (1978) Fluid interaction between granite and sediment during metamorphism, south-central Maine. *American Journal of Science*, 78, 1025–1056.
- Finger, L.W., and Ohashi, Y. (1974a) Preliminary results of the refinement of the crystal structure of holmquistite. *Carnegie Institution of Washington Year Book*, 73, 535–539.
- (1974b) Refinement of the crystal structure of holmquistite. *EOS*, 55, 1201.
- Ginsburg, I.V. (1965) Holmquistite and its structural variety clinoholmquistite. *Trudy Mineralogicheskogo Muzeya Akademii Nauk SSSR*, 16, 73–891 (in Russian).
- Goldich, S.S. (1984) Determination of ferrous iron in silicate rocks. *Chemical Geology*, 42, 343–347.
- Hawthorne, F.C. (1981) Crystal chemistry of the amphiboles. *Mineralogical Society of America Reviews in Mineralogy*, 9A, 1–102.
- (1983) The crystal chemistry of the amphiboles. *Canadian Mineralogist*, 21, 173–480.
- Heinrich, E.W. (1965) Holmquistite and pegmatitic lithium exomorphism. *Indian Mineralogist*, 6, 1–13.
- Irusteta, M.C., and Whittaker, E.J.W. (1975) A three dimensional refinement of the structure of holmquistite. *Acta Crystallographica*, B31, 145–150.
- Karpoff, B.S. (1960) Holmquistite occurrences in the mining property of Quebec Lithium Corporation, Barrante. *International Geological Congress*, 21st, Copenhagen, 1960, pt. 17, p. 7–14.
- Kharaka, Y.K., and Berry, F.A.F. (1973) Simultaneous flow of water and solutes through geological membranes—I. Experimental investigation. *Geochimica et Cosmochimica Acta*, 37, 2577–2603.
- Law, A.D. (1973) Critical evaluation of "statistical best fits" to Mössbauer spectra. *American Mineralogist*, 58, 128–131.
- Leake, B.E. (1978) Nomenclature of amphiboles. *American Mineralogist*, 63, 1023–1053.
- Litvin, A.L., Ginzburg, I.V., Egorova, L.N., and Ostapenko, S.S. (1973) On the crystal structure of holmquistite. *Konstitutsiya; Svoistva Mineralov*, 7, 18–31.
- London, D. (1982) Stability of spodumene in acidic and saline fluorine-rich environments. *Carnegie Institution of Washington Year Book*, 81, 331–334.
- (1986) Holmquistite as a guide to pegmatitic rare-metal deposits. *Economic Geology*, 81, 704–712.

- Munoz, J.L. (1984) F-OH and Cl-OH exchange in micas with applications to hydrothermal ore deposits. *Mineralogical Society of America Reviews in Mineralogy*, 13, 469–493.
- Munoz, J.L., and Ludington, S.D. (1974) Fluorine-hydroxyl exchange in biotite. *American Journal of Science*, 274, 396–413.
- Nabelek, P.I. (1987) General equations for modeling fluid/rock interaction using trace element and isotopes. *Geochimica et Cosmochimica Acta*, 51, 1765–1769.
- Nickel, E.H., Karpoff, B.S., Maxwell, J.A., and Rowland, J.F. (1960) Holmquistite from Barraute, Quebec. *Canadian Mineralogist*, 6, 504–512.
- Norton, J.J. (1976) Field compilation map of the Keystone pegmatite area, Black Hills, South Dakota. U.S. Geological Survey Open-File Map 76–297.
- (1984) Lithium anomaly near Pringle, southern Black Hills, South Dakota, possibly caused by unexposed rare-mineral pegmatite. U.S. Geological Survey Circular 889, 1–7.
- Osann, A. (1913) Ubor Holmquistit, einen Lithiumglaukonphan von der Insel Uto. *Wein Akademie der Wissenschaften Abt. Mathematisch-Physikalische Wissenschaften Abhandlung*, 23, 3–16.
- Page, L.R., Adams, J.W., Erickson, M.P., Hall, W.E., Hanley, J.B., Joralemon, P., Norton, J.J., Pray, L.C., Steven, T.A., Stoll, W.C., and Stopper, R.F. (1953) Pegmatite investigations 1942–1945, Black Hills, South Dakota. U.S. Geological Survey Professional Paper 274, 1–228.
- Papike, J.J., Ross, M., and Clark, J.R. (1969) Crystal chemical characterization of clinoamphiboles based on five new structure refinements. *Mineralogical Society of America Special Paper*, 2, 117–136.
- Papike, J.J., Shearer, C.K., Simon, S.B., and Laul, J.C. (1984) Crystal chemical aspects of Li, Rb, and Cs partitioning between coexisting muscovite and biotite. Abstracts for the 27th International Geological Congress, Moscow, 5, 135.
- Redden, J.A., Norton, J.J., and McLaughlin, R.J. (1982) Geology of the Harney Peak Granite, Black Hills, South Dakota. U.S. Geological Survey Open-file Report 82-481, 18 p.
- Riley, G.H. (1970) Isotopic discrepancies in zoned pegmatites, Black Hills, South Dakota. *Geochimica et Cosmochimica Acta*, 34, 713–725.
- Roberts, W.L., and Rapp, G. (1965) Mineralogy of the Black Hills, South Dakota School of Mines and Technology Bulletin 18, 268 p.
- Robinson, P., Spear, F.S., Schumacher, J.C., Laird, J., Klein, C., Evans, B.W., and Doolan, B.L. (1982) Phase relations of metamorphic amphiboles: Natural occurrences and theory. *Mineralogical Society of America Reviews in Mineralogy*, 9B, 1–227.
- Ross, M., Papike, J.J., and Weiblen, P.W. (1968) Exsolution in clinoamphiboles. *Science*, 159, 1099–1102.
- Ross, M., Papike, J.J., and Shaw, K.W. (1969) Exsolution textures in amphiboles as indicators of subsolidus thermal histories. *Mineralogical Society of America Special Paper*, 2, 275–299.
- Shearer, C.K., Papike, J.J., Simon, S.B., Laul, J.C., and Christian, R. (1984) Pegmatite/wallrock interactions: Black Hills, South Dakota: Progressive boron metasomatism adjacent to the Tip Top pegmatite. *Geochimica et Cosmochimica Acta*, 48, 2563–2580.
- Shearer, C.K., Papike, J.J., and Laul, J.C. (1985) Pegmatite/wallrock interactions, Black Hills, South Dakota: Exomorphic aureoles as indicators of pegmatite fluid composition. *EOS*, 66, 415 p.
- Shearer, C.K., Papike, J.J., Simon, S.B., and Laul, J.C. (1986) Pegmatite-wallrock interactions, Black Hills, South Dakota: Interactions between pegmatite-derived fluids and quartz-mica schist wallrock. *American Mineralogist*, 71, 518–539.
- Sundius, S. (1947) Die chemische Zusammensetzung des Holmquistit. *Geologiska Foereningens i Stockholm Foerhandlingar*, 69, 51.
- Truman, D.L., and Černý, P. (1982) Exploration for rare-element granitic pegmatites. *Mineralogical Association of Canada Short Course Handbook*, 8, 463–493.
- Volfinger, J., and Robert, J.-L. (1980) Structural control of the distribution of trace elements between silicates and hydrothermal solutions. *Geochimica et Cosmochimica Acta*, 44, 1455–1461.
- von Knorring, O., and Hornung, G. (1961) On the lithium amphibole holmquistite, from Benson pegmatite mine, Mtoko, Southern Rhodesia. *Mineralogical Magazine*, 32, 731–735.
- Walker, R.J. (1984) The origin of the Tin Mountain pegmatite, Black Hills, South Dakota. Doctoral thesis, State University of New York at Stony Brook, Stony Brook, New York, 384 p.
- Whittaker, E.J.W. (1969) The structure of the orthorhombic amphibole holmquistite. *Acta Crystallographica*, B25, 394–397.
- Wilkins, R.W.T., Davidson, L.R., and Ross, J.R. (1970) Occurrence and infrared spectra of holmquistite and hornblende from Mt. Marion, near Kalgoorlie, Western Australia. *Contributions to Mineralogy and Petrology*, 28, 280–287.
- Willibey, T.D. (1975) Changes in mineral composition with metamorphism of part of the Oreville Formation, Black Hills, South Dakota. Masters thesis, South Dakota School of Mines and Technology, Rapid City, South Dakota, 62 p.
- Wright, C.M. (1963) Geology and origin of the pollucite-bearing Montgomery pegmatite, Manitoba. *Geological Society of Canada Bulletin*, 74, 919–946.

MANUSCRIPT RECEIVED DECEMBER 29, 1986

MANUSCRIPT ACCEPTED OCTOBER 30, 1987